Title

Nitric oxide release from a photoactive water-soluble ruthenium nitrosyl. Biological effects

Journal

Journal of Coordination Chemistry, 71(11-13)

ISSN

0095-8972

Authors

Crisalli, Meredith A
Franco, Lilian P
Silva, Bruno R
et al.

Publication Date

2018-07-03

DOI

10.1080/00958972.2018.1469129

Peer reviewed

NO Release from a Photoactive Water -Soluble Ruthenium Nitrosyl. Biological Effects.[#]

Meredith A. Crisalli[a,##] *Lilian P. Franco,*[b] *Bruno R. Silva,*[b] *Alda K. M. Holanda* [a,c] *Lusiane M. Bendhack,*[b] *Roberto S. da Silva,*[b,*] *Peter C. Ford*[a,*]

[a] Department of Chemistry and Biochemistry, University of California, Santa Barbara, Santa Barbara, CA 93106 USA.

[b] Faculdade de Ciências Farmacêuticas de Ribeirão Preto, Universidade de São Paulo, Av. do Café s/n, CEP 14040-903, Ribeirão Preto, SP, Brazil.

[c] Departamento de Química Orgânica e Inorgânica, Universidade Federal do Ceará Cx. Postal 12200, Campus do Pici s/n, CEP 60440-900, Fortaleza - CE, Brazil

KEYWORDS: Ruthenium nitrosyl, photochemical release, nitric oxide, myography, cell viability.

ABSTRACT. This research presents the synthesis and characterization of the photochemical nitric oxide (NO) precursor Ru(salenCO_2H)(NO)Cl (**I**, salenCO_2H = N,N'-ethylenebis(3,3'-bis-carboxylsalicylideneiminato). This water-soluble ruthenium nitrosyl releases NO upon photolysis with a quantum yield that is pH dependent owing to the nitrosyl to nitrite conversion of that axial ligand at higher pH. Also described are the water, oxygen, and thermal stability of **I** and the cytotoxicity and the vascular relaxivity properties of **I** in the dark and under photolysis.

[#] This article has been submitted to honor the distinguished career of Prof. Dan Meyerstein.
[##] Taken in part from the Ph.D. Dissertation of MAC, University of California, Santa Barbara, 2015

* Address inquiries to these authors
Roberto S. da Silva. Email: silva@usp.br ; Fax: +55-16-3633-1092
Peter C. Ford. Email: ford@chem.ucsb.edu; Fax: +1-805-893-4120

Introduction

The photochemical "uncaging" of biologically active molecular species has drawn considerable interest [1], since this methodology provides the spatially specific opportunity to release defined concentrations of a substance such as nitric oxide (nitrogen monoxide) at a biological target. This specificity may minimize systemic side-effects while controlling the timing of such an event [2-6]. In this context, we [7-14] and others [15-27] have studied the photochemistry of ruthenium nitrosyl compounds owing to their thermal stability and their photolability toward NO release. Endogenously produced NO demonstrates key bioregulator roles in mammalian physiology (including vasodilation) [28] as well as serving as a cyto-toxin at the higher concentrations generated during immune response to pathogens [29-31]. Moreover, NO is a sensitizer of γ-radiation damage to cells, a feature that could prove valuable in the radiotherapy of hypoxic tumors [32-34]. Application of NO in the latter task is especially attractive given that the concomitant vasodilation should also increase tissue oxygenation at the targeted site and that O_2 is a radiation sensitizer as well. However, due to NO's promiscuous bioactivity, controlling its dosage will be crucial in such therapeutic applications [35], and this provides a major incentive for developing photo-activated NO releasing moieties (photoNORMs) [36].

In this context, we have prepared a new photoNORM Ru(salenCO_2H)(NO)Cl (**1**) (salenCO_2H = N,N'-ethylenebis(3,3'-bis-carboxyl-salicylidene-iminato) that is water soluble, is thermally stable in aerated aqueous media, and is photolabile to NO release. Notably, water solubility adds the challenge of pH dependence to the photoreactivity of **1** owing to the equilibrium between the nitrosyl and N-nitrito forms of this ligand. Although this reversible reaction for ruthenium nitrosyls has long been known [37-41], the present study is to our knowledge, the first to characterize the photoactivated release of NO from such a pH dependent photoNORM system. We also report the activity of **1** in cell toxicity and vascular reactivity studies showing that **1** has moderate cytotoxicity before and after irradiation in cells as well as being able to trigger vasodilation in mammalian aortic rings only in the presence of light with no such effects observed in the dark.

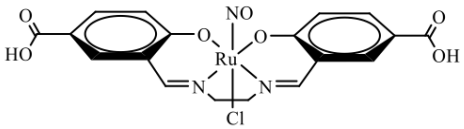

1

Results and Discussion:

The carboxylic acid functionalized ruthenium salen nitrosyl complex Ru(salenCO$_2$H)(NO)Cl (**1**) was prepared according to the reactions outlined in Scheme 1. Details are presented in the Experimental Section.

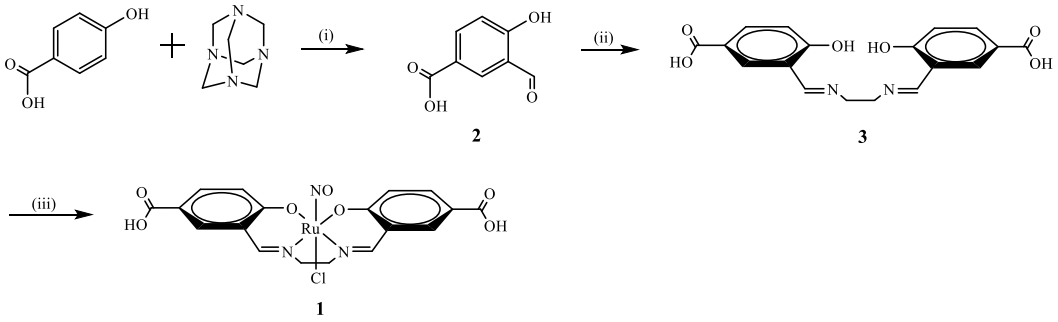

Scheme 1. Synthesis of Ru(salenCO$_2$H)(NO)Cl (1): (i) trifluoroacetic acid, under argon, 4 h reflux; (ii) 0.5 equivalents of ethylenediamine in ethanol, 1 h reflux; (iii) 2.3 equiv. NaH, 1 equiv. Ru(NO)Cl$_3$ • H$_2$O under argon in ethanol 4 h reflux.

The UV-visible spectrum of **1** in aqueous solution is quite sensitive to the pH (Figure 1). These reversible spectral changes can be attributed to two types of reactions, the deprotonation/protonation of the two ligand carboxylic acid groups (Eq. 1) and the acid/base dependent nitrosyl ↔ nitrite conversion described above (Eq. 2). Ruthenium based nitrosyl to nitrite conversions have been studied by a number of researchers [37-41], who demonstrated the reaction of the nitrosyl electrophile (formally represented as Ru^{II}(NO$^+$) in such complexes) with hydroxide.

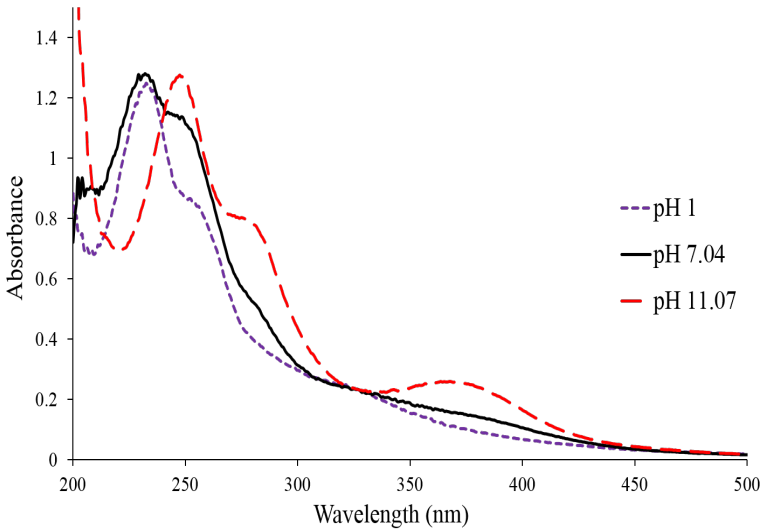

Figure 1. The optical spectra of Ru(salenCO$_2$H)(NO)Cl (**1**) recorded in 50 mM phosphate solution at pH 1.0 (purple short dashes) pH 7.04 (black solid line) and at pH 11.07 (red long dashes). At pH 7.4 the λ_{max} appear at 229 nm (ε = 1.13 x 10^4 M^{-1} cm^{-1}), 248 nm (1.18 x 10^4 M^{-1} cm^{-1}) and ~ 364 nm (2.8 x 10^3 M^{-1} cm^{-1}).

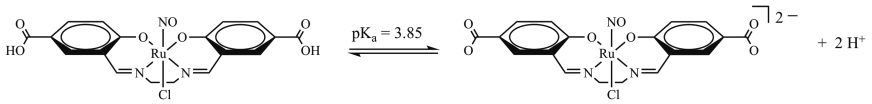

(1)

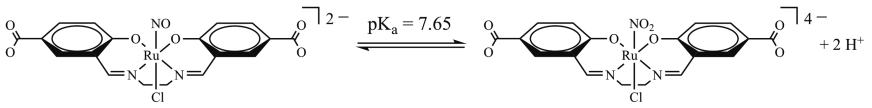

[1-NO]$^{2-}$ **[1-NO$_2$]$^{4-}$**

(2)

The pH dependences of these two transformations in **1** were determined by systematically recording the solution spectrum at 100 separate pH values ranging from 0.5 to 11.5. The carboxylic acid/carboxylate equilibrium(a) (Eq. 1) was(were) evidenced by spectral changes at lower pH values. This was studied quantitatively by plotting the ratio of the absorbance at 247 nm to that at 428 nm (Abs_{277}/Abs_{428}) at pH values from 0.5 to 6. A single inflection in this curve is evident between pH 2.9 and pH 4.3 indicative of a pK_a value of ~3.65 (Figure 2-top). Since only one such inflection was observed, a pKa for a second carboxylic acid is not obvious. Since it is very unlikely that this would occur below 0.5, the more likely explanation is that the first and second carboxylate pK_a values are very close, and the resulting spectral changes for dissociation of the second carboxylic acid occur in tandem at approximately the same pH as those seen for the first carboxylic acid as suggested by Eq. 1. Given that the photochemical and biological experiments reported here were all carried out at pH values significantly above 4, we can assume that under each set of conditions the carboxylates were fully dissociated.

Figure 2-bottom is a plot of the ratio of the absorbance at 371 nm to that at 323 nm (Abs_{371}/Abs_{323}) vs. the solution pH over the range 3.5 to 11.5. This plot displays a clear inflection at pH 7.65, a value that is consistent with the pKa of the nitrosyl/nitrite conversion (Eq. 2) based on earlier observations with analogous ruthenium nitrosyls. The NO^+ to NO_2^- conversion (**[1-NO]$^{2-}$** to **[1-NO$_2$]$^{4-}$**) was also apparent in the aqueous solution phase IR spectrum which showed that the nitrosyl ν_{NO} peak at 1865 cm^{-1} disappears when the solid is dissolved in alkaline solution but reappears when the solution is acidified.

All the pH dependent changes in the UV-visible spectra are reversible, suggesting that the compound does not decompose readily at either low or high pH. This reversibility is consistent with the equilibria shown in Eqs. 1 and 2.

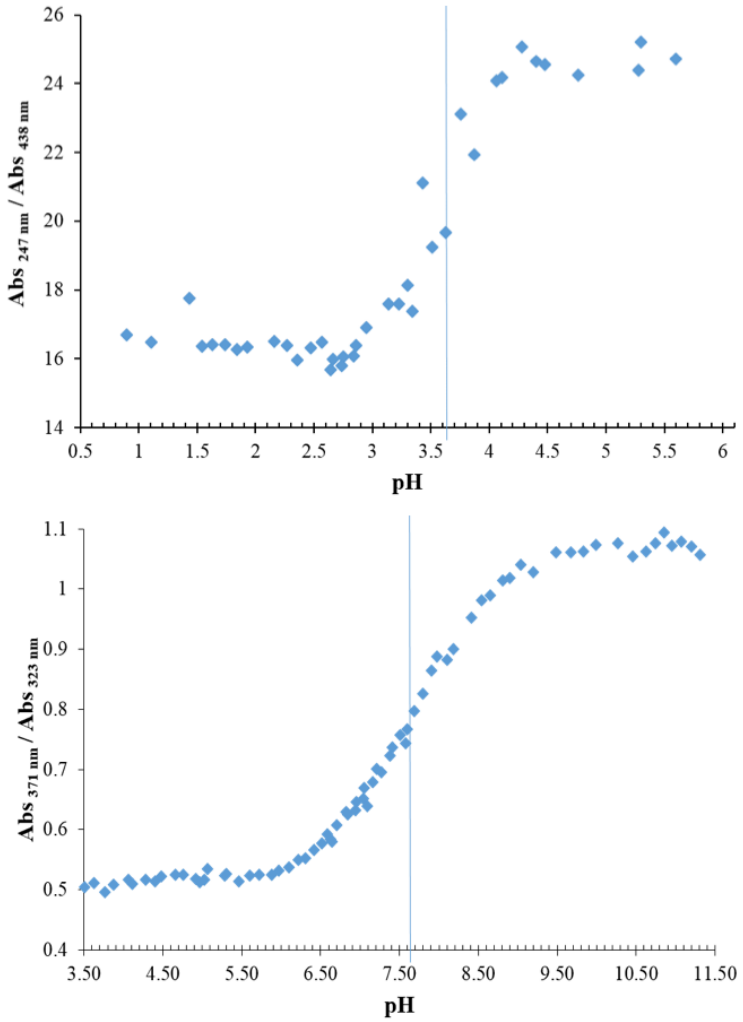

Figure 2. *Top:* Relative absorbance changes for **1** over the pH range 0.5 to 6 plotted as the ratio Abs_{247}/Abs_{438}, where Abs_{247} is the absorbance at 247 nm and Abs_{438} is the absorbance at 438 nm. These are interpreted as indicating the pKa of the carboxylic acid functional group(s) of Ru(salenCO_2H)(NO)Cl. *Bottom:* Spectral titration over the pH range 3.5 to 11.5 of the absorbance ratio Abs_{371}/Abs_{323}, where 371 nm is λ_{max} for the nitrite form and 323 nm is an isosbestic point for all forms of **1**. This is interpreted as reflecting the pH dependence of the N-nitrito/nitrosyl equilibrium for compound **1**. Conditions for both experiements: [**1**] = ~1 x 10^{-4} M in 50 mM KCl solution at 298 K.

Photochemical studies: Photolysis of buffered aqueous solutions of **1** at λ_{irr} = 365 nm led to NO release as detected using a Sievers Nitric Oxide Analyzer (NOA that quantitatively measures NO with high sensitivity. Figure 3 shows a plot of the NO detected (in moles) versus the light absorbed (in Einsteins) by the reactant. This plot is linear with a slope equal to Φ_{NO}. These quantum yields were measured at different pH values in order to assess the effects of the pH-dependent equilibria discussed above. The lower pH results are of particular interest, since the pH of cancer cells falls below 6.8 under hypoxic respiration [42]. NO photolabilization measured in this manner gave the modest Φ_{NO} values (2.6 ±0.3) x10^{-3}, (4.8 ±0.3) x10^{-3} and (5.2±0.2) x10^{-3}

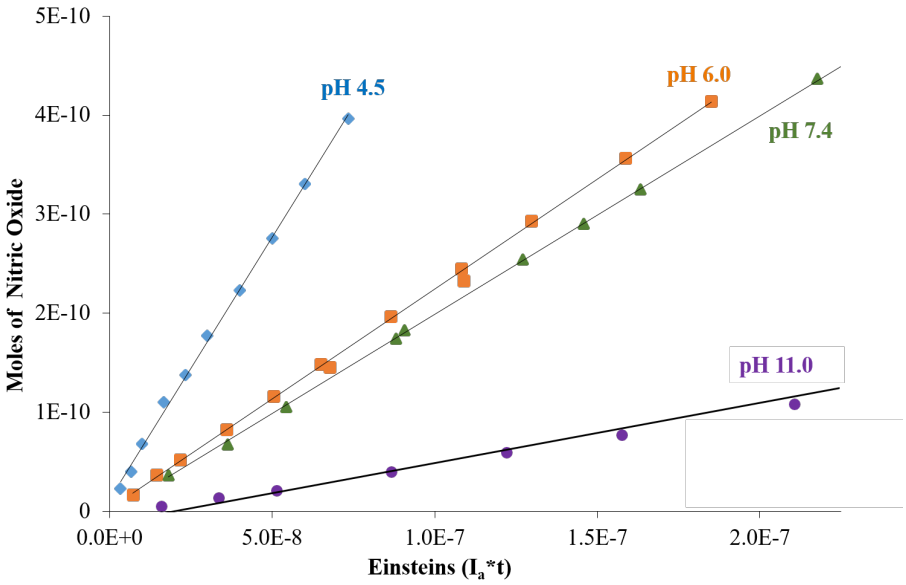

Figure 3. NO release from Ru(salenCO$_2$H)(NO)Cl (**1**) under 365 nm irradiation at pH 4.5 (blue diamond), 6.0 (orange square), 7.4 (green triangle), and 11.0 (purple circle), phosphate buffer solution (50 mM). The plot shows NO (in moles) produced as determined by the NOA verses the light absorbed I_a*t, where I_a is the intensity of the light absorbed in Einsteins per s and t is time in s). The quantum yield Φ_{NO} is the slope of the line and equals 5.3 x10^{-3} (pH 4.5), 2.2 x10^{-3} (pH 6.0), 2.6 x10^{-3} (pH 7.4), and 0.5 x10^{-3} (pH 11.0)

for the respective pH values 7.4, 6.0 and 4.5. In analogy to earlier studies on ruthenium salen nitrosyl complexes [8,10], we interpret the principal photochemical reaction in terms of NO labilization from the nitrosyl form **[1-NO]$^{2-}$** (Eq. 3). Notably, the increased Φ_{NO} values at lower pH correspond to the higher concentrations of the nitrosyl form **[1-NO]$^{2-}$** relative to the N-nitrito analog **[1-NO$_2$]$^{4-}$** as indicated by Eq. 2. Consistent with this view, it is notable that Φ_{NO} is markedly lower at higher pH (0.9 ±0.2) x10^{-3} and (0.5 ±0.1) x10^{-3} at pH 9.0 and pH 11.0, respectively. Thus, it appears that NO photogeneration from the N-nitrito complex is very much less efficient than from the nitrosyl analog, as expected.

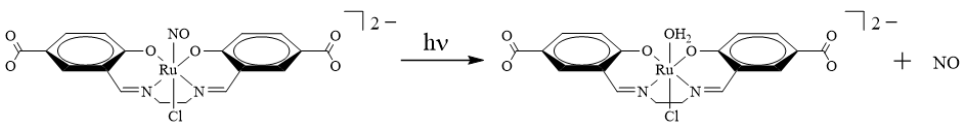

(3)

The Φ_{NO} values for **1** at acidic pH are consistent with that (5 x 10^{-3}) reported previously for the aquo complex [Ru(salen)(H$_2$O)(NO)]Cl (**4**) in aqueous solution when irradiated at 365 nm [10b]. However, both are surprisingly less photolabile than is the simpler, but water insoluble, salen complex Ru(salen)(NO)Cl **(5,** salen = N, N'-ethylenebis(salicylideneiminato)) when irradiated in acetonitrile at 365 nm (Φ_{NO} = 0.13 ± 0.01) [8b]. We don't have a ready explanation for the

>20 fold lower quantum yields for NO release **1** and **4** in buffered aqueous media than from **5** in acetonitrile, unless the solvent H_2O somehow accelerates nonradiative deactivation of the responsible excited state(s). Lehnert and coworkers [27] noted a similar decrease in NO photolability of other ruthenium nitrosyl complexes in aqueous solution and pointed out that such decreases might affect the biological efficacy. The quantum yield for NO release for photolysis carried out at 470 nm with a blue LED is even smaller (Φ_{NO} = 0.2 x 10^{-3} in pH 7.4 buffered solution, SI Fig. S1)

Cellular viability: The cellular toxicity of **1** was studied using the murine melanoma B16F10 cell line. The cells were incubated with concentrations of **1** ranging from 10 μM to 200 μM in Roswell Park Memorial Institute 1640 medium (pH 7.4) and incubated for 4 h. The plates were then irradiated at 470 nm with a blue LED for 4 min or kept in the dark as a control. All plates were then incubated for either 24 or 48 h in the dark. The MTT assay ([40], see Experimental) was performed to evaluate cell viability using wells not containing **1** as the controls (Fig. 4). The cytotoxicity of **1** toward this cell line (B16F10) was moderate under the experimental conditions. For example, there is no statistical difference between the control and the cells incubated with a concentration of 10 μM over 24 h as determined by Tukey's post test with cell viability at 94% and 97% for dark and irradiated samples. However, at much higher concentrations (100 to 200 μM), the cell viability after 24 and 48 h did decrease to the 50-60 % level. For these higher concentration experiments, there were modest, but statistically significant, increases in cell viability for those cultures that had been exposed to light (SI Fig. S2). For example, cells treated 200 μM **1** displayed 51% survival relative to the control after 48 h, while the analogous samples that had been pre-irradiated with the 470 nm light had a 59% survival rate.

Vascular reactivity: Myography experiments were used to test the effect of Ru(salenCO_2H)(NO)Cl on the contraction/dilation of rat aortic rings from which the endothelium layer had been removed to eliminate natural sources of NO generation. These experiments were carried out in pH 7.4 Krebs solution over a large range in the concentration range of **1** by the periodic addition of stock solutions of this compound. The initial [**1**] was 10^{-10} M and the final concentration was 1 x 10^{-4} M. When the system was kept completely in the dark, there was no effect on vascular relaxation at over this concentration range (Fig. 5). In contrast, under ambient room light, some vascular relaxation was noted at [**1**] = 10^{-6} M, while full relaxation was verified when [**1**] equaled 10^{-5} M. However, when a 10^{-5} M solution of **1** was added directly to fresh, fully contracted aortic

rings under ambient light (SI Fig. S-5), full relaxation was slow, requiring ~50 min, owing to the correspondingly slow photoreaction under these conditions. In the absence of light, very little

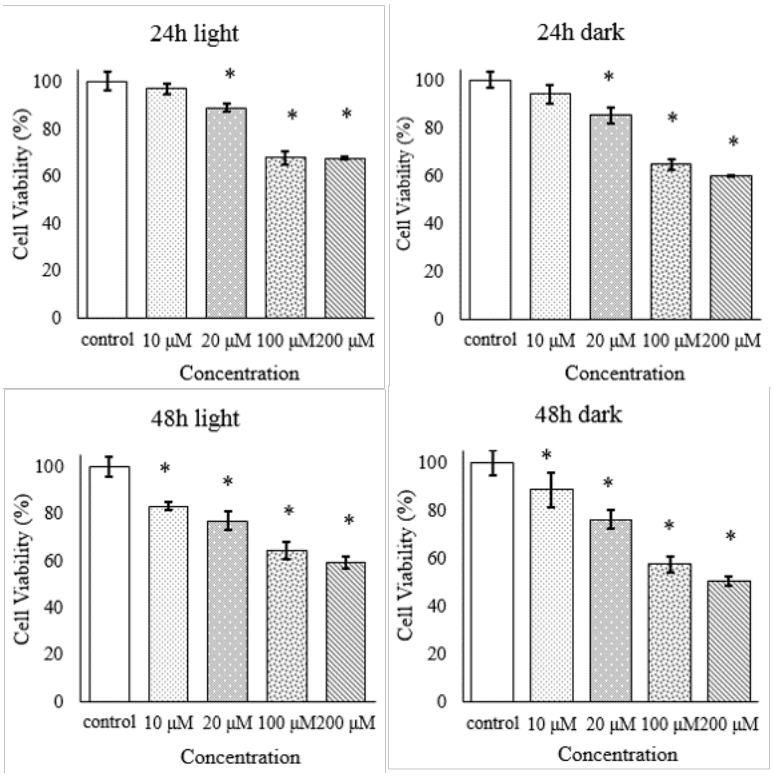

Figure 4. Cell viability plots in different concentrations of compound **1** (Ru(salenCO_2H)(NO)Cl). Cell viability as assessed by the MTT assay (see Experimental). The results show cell survival relative to the control (absence of **1**). The values are the mean ± SEM. * $p < 0.05$ in comparison to others treatments and the control obtained by ANOVA analyses using Tukey's pos test. The plates under light were irradiated for 4 min at 470 nm (4 J/cm^2) at the beginning of the experiment.

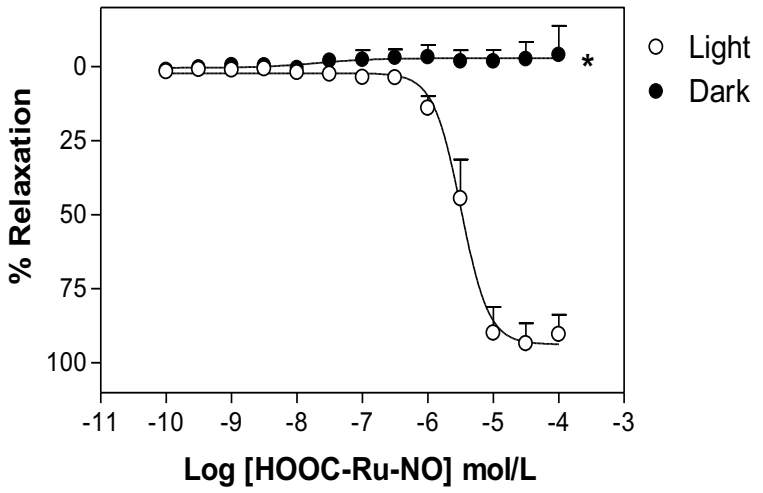

Figure 5. Vascular relaxation induced by Ru(NO)(salenCO_2H)Cl (**1**) in denuded rat aortic rings in ambient light or in the dark. Data are mean ± SEM (n=6).

relaxation was observed, again consistent with the vasodilation process generally being triggered by the activation of the very sensitive enzyme guanylyl cyclase [31]. The areas under these curves were used to calculate the relative relaxation induced by **1** over 60 min in the dark and under ambient light (SI Fig. S3). Notably, for the latter experiment, there was little significant difference in the responses seen for thoracic aortas with their endothelium intact vs. those that have been denuded. Thus, the vascular dilation observed under ambient light can be attributed to the NO released by photolabilization from the ruthenium nitrosyl and not by residual NO from endogenous production in the system.

Chemical and electrochemical reduction: Ruthenium nitrosyl complexes have also been shown to release NO upon one electron reduction (Eq. 4) [44]. This type of release was tested with Ru(salenCO_2H)(NO)Cl electrochemically, and it was found that in order to induce the production of NO, **1** required a charging potential at –0.5 V vs Ag/AgCl. Differential pulse voltammograms of **1** in aqueous solution shows the peak at –0.3 V *vs* Ag/AgCl attributed to $\{Ru\text{-}NO\}^{2+/3+}$ oxidation after such charging. The initial reduction with similar systems has been identified as centered on the nitrosyl ligand, which can be represented as follows: $Ru^{II}(NO^{+}) + e^{-} \rightarrow Ru^{II}(NO\bullet)$ [44]. Pre-treatment at –0.5 V causes the decrease in the peak intensity at –0.3 V (Fig. 6) consistent with labilization of the NO ligand upon reduction of **1** (Eq. 4). A second peak at ~ 0.1 V *vs* Ag/AgCl appears after the reduction process, which was attributed to the oxidation of the aquo species Ru(salenCO_2H)(H_2O)Cl, **[1-H_2O]$^{3-}$**, which is formed upon NO labilization from reduced **1**. Thermal release of NO from reduced **1** was qualitatively confirmed by using a NO specific

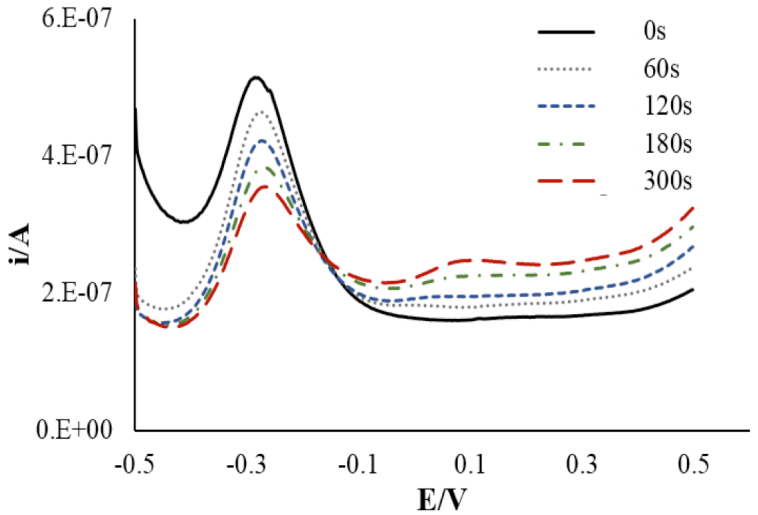

Figure 6. Differential pulse voltammetry scans with carbon glass electrode with Ag/AgCl reference electrode of Ru(salenCO_2H)(NO)Cl (**1**). Scans recorded after specified timed charging with conditioning potential of -0.5 V and run between –0.5 and 0.5 V.

electrode (SI Fig. S4). The time dependence of the scans in Figure 5 as well as for the formation of free NO suggest that thermal release of NO from the reduced **1** (Eq. 4) has a half-life of several hundred seconds.

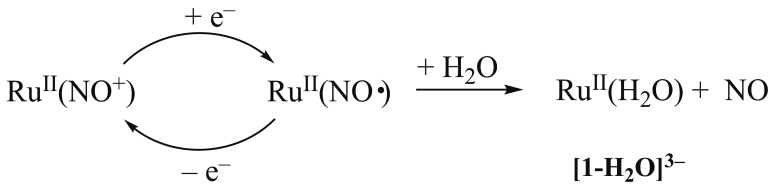

(4)

The addition of ascorbate (0.14 M) to a solution of **1** (28 μM) in pH 7.4 phosphate buffer also triggers NO release as demonstrated using the NO specific electrode system (SI Fig. S-6).

Summary:

This study has described a photo-activated NO releasing moiety Ru(salenCO_2H)(NO)Cl (**1**) that is stable in aerobic aqueous solutions while displaying pH dependent quantum yields for NO generation *in vitro*. This complex was shown to stimulate vasodilation in mammalian aortic rings specifically when exposed to ambient light. The pH dependent quantum yields can be attributed to the nitrosyl / N-nitrito equilibrium that results in enhanced NO release at lower pH. Such an effect suggests a strategy for targeting NO release in the relative acidic environment characteristic of hypoxic tumors [45,46]. Neither the photoNORM precursor nor the small amount of NO released is cytotoxic, but the photo-induced NO release, even with a very modest quantum yield, would be sufficient to trigger soluble guanylyl cyclase mediated vasodilation [47], thereby increasing circulation to and oxygenation of the targeted tissues. If this process were coupled to radiotherapy, the increased oxygenation would enhance the sensitivity of the targeted tissues to radiation-induced cell death. Similarly, such targeted NO release leading to enhanced circulation could synergistically enhance the efficacy of chemotherapy.

Nonetheless, a realistic evaluation of the present system has to take into consideration that the short wavelength necessary to trigger NO release from 1 would have poor penetration through living tissue. For this reason, strategies that can utilize tissue penetrating near infrared (NIR) light

such the use of antennas such as upconverting nanoparticles that can be activated by multiphoton NIR excitation need to be employed. Notably, the pendant carboxylate groups of **1** besides providing aqueous solubility, also provide ample opportunity for further conjugation with groups like cell-targeting peptide [48] or with antennas such as nanomaterials with desirable photophysical properties [13,49]. These studies are ongoing.

Experimental Section.

Materials*:* Trichloridonitrosylruthenium(III) monohydrate, $Ru(NO)Cl_3 \bullet H_2O$ was purchased from Strem Chemicals Inc. Other synthetic materials including trifluoroacetic acid, 4-hydroxybenzoic, hexamethylenetetramine, 95% sodium hydride and laboratory solvents were purchased from Sigma-Aldrich. Cell lines, media, and MTT assay reagents for cell toxicity studies were provided by the Faculdade de Ciências Farmacêuticas de Ribeirão Preto, Universidade de São Paulo. All buffers used for quantum yield measurements were prepared in nanopure water at 50 mM concentrations. The pH was adjusted to exact values using dilute NaOH or HCl as required. Phosphate buffers were prepared for pH values 11.0, 7.4, 6.0, and 4.5 while tris(hydroxymethyl)aminomethane (Tris) was used to prepare the pH 9.0 buffer.

Synthesis of Ru(salen-CO_2H)(NO)Cl (1). The salen-CO_2H ligand (**3**) was prepared according to the reaction sequence outlined in Scheme 1 from salicylaldehyde-4-carboxylic acid (**2**), which was synthesized according to published procedures [50] (See SI). The nitrosyl complex chloridonitrosyl(N,N'-ethylenebis(3,3'-bis-carboxylsalicylidene-iminato)ruthenium(III) (**1**) was prepared from **3** as follows. A mixture of **3** (0.50 g, 1.41 mmoles), sodium hydride (0.107 g, 4.45 mmoles), and trichloridonitrosylruthenium(III) monohydrate, $Ru(NO)Cl_3 \bullet H_2O$, (0.317 g, 1.41 mmoles) was added to a three neck 300 mL round bottom flask and placed under an argon atmosphere. Approximately 150 mL of deaerated ethanol was then transferred via cannula into the reaction flask. The resulting solution was refluxed under argon in the dark for 4 h, after which it was allowed to cool to room temperature, and the ethanol was removed via rotary evaporation. The sodium chloride byproduct was removed from the desired product by washing the solid with water adjusted to pH 5 with dilute HCl. The remaining solid was dried under vacuum for several hours (**Scheme 1**, step iii) (89% Yield). ^{1}H NMR (DMSO-d_6): δ 8.69ppm (1H, s) aldimine protons, 8.02

(1H, s), 7.85 (1H, d), 6.83 (1H, d) phenyl protons, 3.94 (2H, s) ethylene bridge. Analysis: Theoretical for [Ru(salenCO_2H)(NO)Cl]•2H_2O ($C_{18}H_{16}N_3O_7ClRu$•2H_2O): C, 38.68%; H, 3.61%; N, 7.52%. Found: C, 38.3%; H, 3.43%, N 7.59%. FTIR (KBr) ν_{NO} = 1865 cm^{-1}. UV-vis (pH 7.4 in 50 mM phosphate buffer): λ_{max} 248 nm (ε = 3.8 x 10^4 M^{-1} cm^{-1}), 359 (ε = 6.6 x 10^3 M^{-1} cm^{-1}).

Once the product was washed with the pH 5 solution, solubility for aqueous solution experiments was achieved by dissolving the compound into a solution above pH 9. These stock solutions were then diluted into buffered media for spectroscopic studies or for investigation with murine tissues or cells.

Quantum yield measurements: NO release was measured using a GE model NOA 280i Sievers Nitric Oxide Analyzer (NOA) calibrated per the manufacturer's specifications. This device quantitatively measures the NO present in a carrier gas, which is either helium or medical grade air, that is entrained through the photolysis solution [51]. The carrier gas was first passed through a glass chamber containing only solvent prior to entering the reaction cell in order to prevent evaporative solvent loss and to maintain a constant volume in the reaction cell throughout the experiment. Quantum yield measurements at the pH values at 4.5, 6.0, 7.4, 9.0, and 11.0 were conducted individually using a stock solution of **1**. The cuvette was filled with 3 mL of pH-adjusted solutions of **1** and entrained with carrier gas for 5 min, in order to allow the NOA establish a stable baseline. The photolysis was conducted at λ_{irr} 365 nm with the light from a high-pressure mercury lamp passed through a narrow band pass interference filter or at λ_{irr} 470 nm with a blue LED from Luxeon. The intensity of the excitation at 365 nm was determined using ferrioxolate actinometry [52], and the intensity of the LED light was measured with a Newport power meter. Individual samples were irradiated for varied time intervals controlled by a Uniblitz shutter and the photochemically released NO was recorded using the NOA software "Liquid". The plotted slope is Φ_{NO} (see Fig. 3).

pKa measurements: The pH dependent changes in UV-visible spectrum of **1** were recorded in order to examine the acid/base dependent equilibria. In order to determine these quantitatively, compound **1** was dissolved in slightly basic water and diluted to a concentration of 0.15 mM in 50 mM KCl solution. The pH was adjusted by adding small increments of dilute hydrochloric acid and determined with a pH meter. After the pH stabilized, the UV-visible spectrum was recorded. This was done for ~100 different pH values from 0.5 to 11.

Cell viability studies: The cytotoxicity activity of **1** was evaluated against B16F10 murine melanoma cells using the colorimetric method with 3-(4,5-dimethylthiazol-2-yl)-2,5-diphenyltetrazolium bromide (MTT assay) [43]. The cells were cultured in Roswell Park Memorial Institute 1640 medium (RPMI) enriched with 2% fetal bovine serum, seeded into 96-well plates (2×10^5 cells/well) and incubated according to published procedures [53]. Stock solutions of **1** were prepared in concentrations of 20 mM, 10 mM, 2 mM, and 1 mM, and 2 μL aliquots of these solutions were added to each well to obtain a total volume of 200 μL of media. The final concentrations of **1** in the wells were 200 μM, 100 μM, 20 μM, 10 μM, and 0 μM (control). The cells were incubated with **1** in the dark for 4 h in the RPMI medium (pH 7.2). Phenol red indicator was not used in the media during the photolysis to avoid light being absorbed by this indicator. Half of the cell plates were irradiated with 470 nm light for 4 min with a modified cell plate LED, and all plates were then incubated for either 24 or 48 h. After the incubation, the media was removed and 200 μL MTT solution (0.5 mg/mL RPMI medium) was added to each well and incubated for 3 h. MTT is converted into crystals by the viable cells. To solubilize the product, the medium was removed and 200 μL of DMSO was added into the wells. (MTT solution; 12 mM thiazolyl blue tetrazolium bromide in phosphate buffer was diluted in media to a final concentration of 1.2 mM.) The absorbance was recorded by a Thermo Plate leitora de microplaca TP-reader plate reader at 570 nm. The reported values are an average of triplicate samples in three different experiments. The data was normalized to the control wells, not containing compound **1**. Data was compiled and processed using Prism 5.0 software.

Vascular dilation studies: *All the procedures were performed in accordance with the standards and policies of Animal Care and Use Committee of the University of São Paulo.* Male rats (180-200 g) were sacrificed by decapitation under anesthesia. The thoracic aorta was quickly removed, and cut into rings (4-5 mm length). The endothelium was mechanically removed from one of the two rings by gently rolling the lumen of the vessel on a thin wire. Aortic rings with and without endothelium cells were studied concurrently. The aortic rings were placed between two stainless-steel stirrups and connected to an isometric force transducer (Letica Scientific Instruments, Barcelona–Spain) to measure tension in the vessels. The rings were placed in an organ chamber containing Krebs solution with the following composition (mM): NaCl (130.0), KCl (4.7), KH_2PO_4 (1.2), $MgSO_4$ (1.2), $NaHCO_3$ (14.9), glucose (5.5) and $CaCl_2$ (1.6). The solution was maintained at pH 7.4 and bubbled with a gas mixture of 95% O_2 and 5% CO_2 at 37 °C. The

rings were initially stretched to a basal tension of 1.5 g and allowed to equilibrate for 60 min. The presence of endothelium was evaluated by the degree of relaxation induced by acetylcholine (1 μM) in the presence of contractile tone induced by phenylephrine (PE, 0.1 μM). Endothelium-intact arteries were discarded if relaxation with acetylcholine was not greater than 80% while endothelium-denuded arteries were discarded if there was degree of relaxation for acetylcholine higher than 10%. The rings were then washed and pre-contracted with 10 μL of PE (0.1 μM). After stabilized contraction, two tests for vascular relaxation were separately conducted using compound **1**: the concentration-effect curve and the time course with the necessary concentration to induce maximum vascular relaxation. For the concentration-effect curve, stock solutions from 0.1 μM - 5 mM were prepared and cumulatively added in sequence to the Krebs buffered organ chambers. The final concentration ranged from 10^{-10} M to 10^{-4} M (Figure 4). The time course for compound **1** induced relaxation was monitored over the course of an hour following the single administration of 20 μL of 5 mM **1** for a final concentration of 10^{-5} M. (Figure 5). Both experiments were conducted in ambient light or dark. The comparisons between groups were assessed by student *t*-test. The level of statistical significance was defined as $P<0.05$.

Voltammetric studies: The electrochemical study was performed with an AUTOLAB PGSTAT 30 model potentiostat galvanostat consisting of a conventional three electrode cell with a platinum wire auxiliary electrode, an Ag/AgCl reference electrode, and a glassy carbon working electrode. An aqueous 0.1 M KCl solution was used as the supporting electrolyte. The solution was charged at -0.5 V for a period of 0 and 300 s prior to scanning from -0.5 V- 0.5 V. Additionally, negative scan was charged at 0.3 then run over from 0.3 - -0.5 V.

Author Contributions

The manuscript was written through contributions of all authors. All authors have given approval to the final version of the manuscript.

Abreviations used:

Abs: absorbance

LED: light emitting diode

λ_{irr}: wavelength of irradiation

MTT: 3-(4,5-dimethylthiazol-2-yl)-2,5-ditetrazolium bromide

NIR: near infrared

NOA: Sievers Nitric Oxide Analyzer

PE: phenylephrine

photoNORM: photo-activated nitric oxide releasing moiety

Φ_{NO}: quantum yield for nitric oxide release

RPMI medium: Roswell Park Memorial Institute 1640 medium

salenCO_2H: N,N'-ethylenebis(3,3'-bis-carboxyl-salicylidene-iminato

SI: supporting information

UV-vis: ultraviolet-visible

Acknowledgments:

This research was supported by the US National Science Foundation (CHE-1058794 and CHE-1405062) for work completed in the US and by the Brazilian agencies Conselho Nacional de Desenvolvimento Científico e Tecnológico (CNPq), Coordenação de Aperfeiçoamento de Pessoal de Nível Superior (CAPES) and Fundação de Amparo à Pesquisa do Estado de São Paulo (FAPESP) for work completed in Brazil. M.A.C. thanks the ConvEne-IGERT program at UCSB (NSF-DGE 0801627) for a fellowship and for travel support to carry out experiments in Brazil.

Supporting Information: Three pages with 4 additional figures and the synthesis of the ligand salenCO_2H

References

[1] H. M. Lee, D. R. Larson, D. S. Lawrence, *ACS Chem. Biol*. **4**, 409–427 (2009).
[2] P. C. Ford, J. Bourassa, K. M. Miranda, B. Lee, I. Lorkovic, S. Boggs, S. Kudo, L. Laverman, *Coord. Chem. Rev*. **171**, 185-202 (1998).
[3] (a) P. C. Ford, *Acc. Chem. Res*. **41**, 190–200 (2008). (b) P. C. Ford *Nitric Oxide***. 34,** 56-64 (2013).
[4] H.-J. Xiang, M. Guo, J.-G. Liu, *Europ. J. Inorg. Chem*. **12,** 1586-1595 (2017).
[5] A. D. Ostrowski, P. C. Ford, *Dalton Trans*. **38**, 10660-10669 (2009).
[6] S. Sortino, *J. Mater. Chem.* **22**, 301−318 (2012).
[7] I. M. Lorkovic, K. M. Miranda, B. Lee, S. Bernhard, J. R. Schoonover, P. C. Ford, *J. Am. Chem. Soc.* **120**, 11674-11683 (1998).
[8] (a) C.F. Works, P.C. Ford, *J. Am. Chem. Soc.* **122**, 7592–7593 (2000). (b) C.F. Works, C.J. Jocher, G.D. Bart, X. Bu, P.C. Ford, *Inorg. Chem.* **41**, 3728–3739 **(**2002).
[9] R.M. Carlos, A.A. Ferro, H.A.S. Silva, M.G. Gomes, S.S.S. Borges, P.C. Ford, E. Tfouni, D.W., Franco, *Inorg. Chim. Acta* **357**, 1381-1388 (2004).
[10] (a) E. Tfouni, J. Bordini, P.C. Ford, *Chem. Commun.* 4169-4171 (2005). (b) J. Bordini, D.O. Novaes, I. E. Borissevitch, B.T. Owens, P.C. Ford, E. Tfouni, *Inorg. Chim. Acta* **361**, 2252-2258 (2008).

[11] (a) F.d.S. Oliveira, V. Togniolo, T.T. Pupo, A.C. Tedesco, R. S. da Silva, *Inorg. Chem. Commun.* **7**, 160-164 (2004). (b) C.N. Lunardi, A.L. Cacciari, R. Santana da Silva, L.N. Bendhack, *Nitric Oxide-Biology and Chemistry,* **15,** 252-258 (2006). (c) L. C. B Ramos, M. S. P. Pereira; D. Callejon, M. Baruffi, C. N. Lunardi, L. D. Slep, L. M. Bendhack, R. S. da Silva, *Europ. J. Inorg. Chem*. **22**, 3592-3597 (2016)
[12] B. Birkmann, S. Bandyopadhyay, B.T. Owens, G. Wu, P.C. Ford, *J. Inorg. Biochem.* **103**, 237-242 (2009).
[13] L P. Franco, S. A. Cicillini, J. C. Biazzotto, M. Schiavon, A. Mikhailovsky, P. Burks, J. Garcia, P. C. Ford, R. S. da Silva, *J Phys. Chem. A* **2014**, *118*, 12184-12191.
[14] G. Nakamura, M. Kondo, M. Crisalli, S. K. Lee, A. Shibata, P. C Ford, S. Masaoka, *Dalton Transactions* **44**, 17189-17200 (2015).
[15] (a) A.A. Ferro, R.M. Carlos, H.A.S. Silva, M.G. Gomes, S.S.S. Borges, E. Tfouni, D.W. Franco, *Nitric Oxide-Biology and Chemistry* **6**, 387 (2002). (b) E. Tfouni, M. Krieger, B.R. McGarvey, D.W. Franco, *Coord. Chem. Rev*. **236**, 57-69 (2003).
[16] E. Tfouni, F.G. Doro, L.E. Figueiredo, J.M.C. Pereira, G. Metzker, D.W. Franco, *Curr. Med. Chem.* **17**, 3643-3657 (2010).
[17] (a) A.K. Patra, P.K. Mascharak, Inorg. Chem. **42**, 7363-7365 (2003). (b) N.J. Fry, J. Wei, P.K. Mascharak, *Inorg. Chem.* **50**, 9045-9052 (2011). (c) T. R. deBoer, P. K. Mascharak, *Adv. Inorg. Chem*. **67** ,145-170 (2015)
[18] (a) K. Ghosh, S. Kumar, R. Kumar, U. P. Singh, N. Goel, *Inorg. Chem.* **49**, 7235-7237 (2010). (b) A. Kumar, R. Pandey, R.K. Gupta, K. Ghosh, D.S. Pandey, *Polyhedron* **52**, 837-843 (2013).
[19] A. Fraix, S. Sortino *Chemistry-An Asian J*. **10**, 1116-1125 (2015)
[20] Becker, S. Kupfer, M. Wolfram, H. Goerls, U. S. Schubert, E. V. Anslyn, B. Dietzek, S. Graefe, A. Schiller, *Chemistry- Eur. J.* **21**, 15554 (2015)
[22] T. Q. Deng, H.-J. Xiang, W.-W. Tang, *J. Inorg. Biochem*. **165**, 152-158 (2016)
[23] S**.** Amabilino, M. Tasse, P. G. Lacroix, S. Mallet-Ladeira, V. Pimienta, J. Akl, I. Sasaki, I. Malfant, *New. J. Chem.* **41**, 7371-7383 (2017)
[24] Y. H**.** Li, M. Guo, S.-W. Shi, Q. L. Zhang, S.-P. Yang, J. G. Liu, Jin-Gang, *J. Mater. Chem. B*, **5**, 7831-7838 (2017)
[25] R. Prakash, A. U. Czaja, F. W. Heinemann, D. Sellmann. *J. Am. Chem. Soc.* **127**, 13758-13759 (2005).
[26] P. De, B. Sakar, S. Maji, A. K. Das, E. Bulak, S. M. Mobin, W. Kaim, G. K. Lahiri. *Eur. J. Inorg. Chem.*, **2009**, 2702-2710 (2009)
[27] A. C. Merkle, A. B. McQuarters, N. Lehnert, *Dalton Transactions* **41**, 8047-8059 (2012)

[28] P.L. Feldman, O.W. Griffith, H. Hong, D.J. Stuehr, *J. Med. Chem*. **36**, 491-496 (1993).
[29] D.A. Wink, I. Hanbauer, M.B. Grisham, F. Laval, R.W. Nims, J. Laval, J. Cook, R. Pacelli, J. Liebmann, M. Krishna, P.C. Ford, J. B. Mitchell, *Curr. Top. Cell. Regul*. **34**, 159-187 (1996).
[30] D.A. Wink, J.B. Mitchell, Free *Radical Biol. Med.* **25**, 434−456 (1998).
[31] L.J. Ignarro, Ed. *Nitric Oxide: Biology and Pathobiology*, 2nd ed.; Elsevier Inc.: Burlington, MA, 2010.
[32] J.B. Mitchell, D.A. Wink, W. DeGraff, J. Gamson, L.K. Keefer, M.C. Krishna, *Cancer Res*. **53,** 5845−5848 (1993)
[33] J. Bourassa, W. DeGraff, S. Kudo, D.A. Wink, J.B. Mitchell, P.C. Ford, *J. Am. Chem. Soc*. **119,** 2853−2860 (1997).
[34] B.F. Jordan, P. Sonveaux, O. Feron, V. Gregoire, N. Beghein, C. Dessy, B. Gallez, I*nt. J. Cancer* **109**, 768−773 (2004).
[35] D.A. Wink, H.B. Hines, R.Y.S. Cheng, C.H. Switzer, W. Flores-Santana, M.P. Vitek, L.A. Ridnour, C.A. Colton, *J. Leukocyte Biol*. **89,** 873-891, (2001)
[36] A.E. Pierri, D.A. Muizzi, A.D. Ostrowski, P.C. Ford, *Structure & Bonding*, **165**, 1-45 (2015).
[37] J.B. Godwin, T.J. Meyer *Inorg. Chem*., **10**, 2150–2153 (1971).

[38] (a) G.F. Caramori, A.G. Kunitz, K.F. Andriani, F.G. Doro, G. Frenking, E. Tfouni, *Dalton Trans*. **41**,7327-7339 (2012). (b) M. G. de Oliveira, F. F. Doro, E. Tfouni, M. H. Krieger, *J. Pharm. Pharmacol*. **69**, 1155-1165 (2017)
[39] F. Bottomley, P.S. Braterman Eds., *Reactions of Coordinated Ligands,* vol. 2, Plenum Press, New York, 1989.
[40] F. Roncaroli, M.E. Ruggiero, D.W. Franco, G.L. Estiu, J.A. Olabe, *Inorg. Chem*. **41,** 5760 (2002).
[41] N.O. Codesido, T. Weyhermüller, J.A. Olabe, L.D. Slep, *Inorg. Chem*. **53**, 981-997 (2014).
[42] C.W. Song, R. Griffin, H.J. Park, *Cancer Drug Discovery and Development: Cancer Drug Resistance,* p. 21- 42, Ed. B. Teicher Humana Press Inc., Totowa, NJ, 2006
[43] T.J. Mosmann, *J. Immunological Methods* **65,** 55–63 (1983).
[44] D.R. Lang, J.A. Davis, L.G.F. Lopes, A.A. Ferro, L.C.G. Vasconcellos, D.W. Franco, E. Tfouni, A. Wieraszko, M.J. Clarke, *Inorg. Chem*. **39**, 2294(2000).
[45] P. Vaupel, Seminars *Radiat. Oncol*. **14**, 198-206 (2004).
[46] H. Bruye`re, A.D. Westwell, A.T. Jones, *Bioorg. Med. Chem*. **20**, 2200–2203 (2010).
[47] J. Garthwaite, Mol. *Cell. Biochem.* **334**, 221-232 (2010).
[48] E.S. Levy, D.P. Morales, J.V. Garcia, N.O. Reich, P.C. Ford, *Chem. Commun*. **51**, 17692-17695 (2015)
[49] D. Neuman, A.D. Ostrowski, A.A. Mikhailovsky, R.O. Absalonson, G.F. Strouse P.C. Ford, *J. Am. Chem. Soc*. **130,** 168-175 (2008**)**
[50] V. Béreau, V. Jubéra, P. Arnaud, A. Kaiba, P. Guionneau, J.-P. Sutter, *Dalton Trans.* **39**, 2070-2077 (2010)
[51] "Photochemical Studies on Cr(III) Cyclam Complexes. Photosensitization with Semiconductor Quantum Dots and Nitric Oxide Release". A.D. Ostrowski, Ph.D. Dissertation, UC Santa Barbara, July 2010.
[52] J.G. Calvert , J.N. Pitts, Jr., *Photochemistry*, John Wiley, New York, 1966, pp780-815.
[53] Z.A. Carneiro, J.C.B. de Moraes, F.P. Rodrigues, R.G. de Lima, C. Curti, Z. Novais da Rocha, M. Paulo, L. M. Bendhack, A. C. Tedesco, A. L. B. Formiga, R. S. da Silva, *J. Inorg. Biochem.* **105**, 1035-1043 (2011).

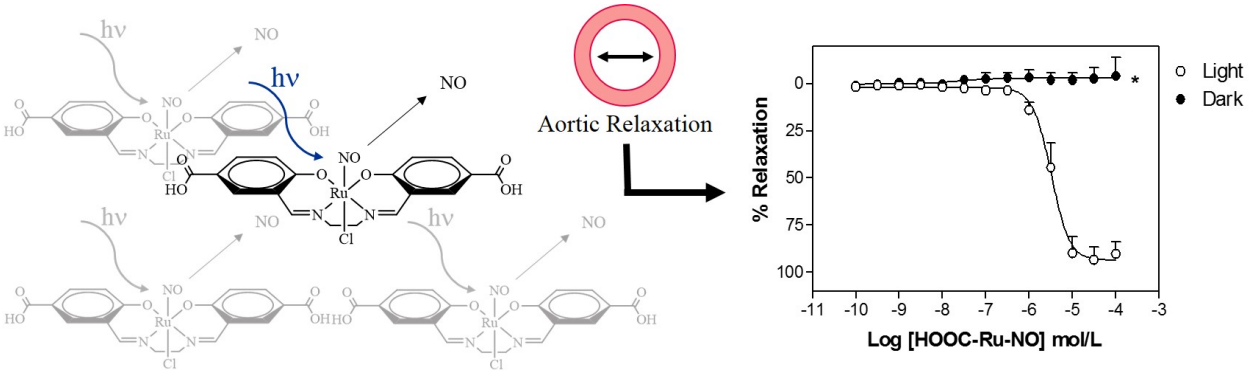

Synopsis:

The water-soluble photochemical nitric oxide (NO) precursor Ru(salen-CO2H)(NO)Cl (salen-CO2H = N,N'-ethylenebis(3,3'-bis-carboxylsalicylideneiminato) displays a pH dependent quantum yield owing to the nitrosyl/ N-nitrito equilibrium of the axial ligand.